Vortex states in a two-dimensional superconductor at high magnetic field in a periodic pinning potential

V. Zhuravlev[1] and T. Maniv[1,2,*]
[1]*Chemistry Department, Technion-Israel Institute of Technology, Haifa 32000, Israel*
[2]*Grenoble High Magnetic Field Laboratory, Max-Planck-Institut für Festkorperforschung, and Center National de la Recherche Scientific, 25 Avenue des Martyres, F-38042, Cedex 9, France*
(Received 25 May 2003; published 6 November 2003)

The effect of a periodic pinning array on the vortex state in a two-dimensional superconductor at low temperatures is studied within the framework of the Ginzburg-Landau approach. It is shown that an attractive interaction of vortex cores to a commensurate pin lattice stabilizes vortex solid phases with long-range positional order against violent shear fluctuations. Exploiting a simple analytical method, based on the Landau orbital description, we derive a rather detailed picture of the low-temperature vortex-state phase diagram for the first matching magnetic field. It is predicted that for sufficiently clean samples application of an artificial periodic pinning array would enable one to directly detect the intrinsic shear stiffness anisotropy characterizing the ideal vortex lattice.

DOI: 10.1103/PhysRevB.68.174507 PACS number(s): 74.20.De, 74.25.Dw, 74.25.Qt

I. INTRODUCTION

The nature of the vortex lattice melting transition in two-dimensional (2D) superconductors has been debated in the literature for many years.[1] Early proposals,[2,3] based on the similarity to the Kosterlitz-Thouless-Halperin-Nelson-Young theory of melting in 2D solids,[4] have led to the conclusion that the melting transition is continuous. A weak first-order melting transition was predicted more recently, however, by several Monte Carlo simulations[5,6] using the Ginzburg-Landau (GL) theory. It has been shown recently[1,7,8] that shear motions of Bragg chains along the principal crystallographic axis of the vortex lattice cost a very small fraction of the superconducting (SC) condensation energy and are responsible for the low-temperature vortex lattice melting.

This intrinsic anisotropy of the vortex lattice with respect to shear stress cannot be easily detected experimentally since the orientation of the principal axis with respect to the laboratory frame depends on the local pinning potential, which in real superconductors is usually produced by a random distribution of pinning centers. Indirect experimental detection of this hidden anisotropy may be achieved by means of the small-angle neutron scattering (SANS) technique, due to the 1D nature of the effective thermal fluctuations in the vortex liquid state just above the melting point (see Ref. 8). A direct detection of this anisotropy (e.g., by means of SANS) could be possible if vortex solid phases with long-range positional order were stabilized against the random influence of pinning impurities. This can be achieved by exposing the SC sample to an artificial periodic pinning array and tuning the magnetic flux density to an integer multiple of the pinning center density. As will be shown in this paper, under certain conditions the artificial periodic pinning potential can stabilize weakly pinned vortex solid phases with long-range positional order, which may exhibit the shear stiffness anisotropy characterizing an ideal vortex lattice.

Vortex matter interacting with periodic pinning arrays is currently a subject of intense experimental[9–16] and theoretical[17–23] investigations. Developments of nanoengineering techniques, such as *e*-beam lithography, make it possible to fabricate well-defined periodic arrays of submicron antidotes, or magnetic dots, in SC films with low intrinsic pinning, enabling to study the effect of well-controlled artificial pinning centers. These experiments have shown that under certain conditions the underlying artificial pinning centers can attract vortices very strongly, thus stabilizing vortex patterns with global translational symmetry against the random influence of the natural pinning centers.

From a theoretical point of view utilization of an external periodic pinning potential provides a convenient tool for testing different models of the vortex state by simplifying considerably the model calculations. At the same time, however, the interplay between the vortex-vortex interactions, which favor hexagonal vortex lattice symmetry, and the underlying periodic potential can lead to a variety of vortex configurations, depending on the pinning strength, in which vortices detach from pinning centers to form more closely packed vortex patterns.

As the interaction with a periodic substrate stabilizes the vortex system versus thermal fluctuations, it generally increases the melting temperature. However, as we shall see in this paper, deviation from the ideal hexagonal symmetry due to pinning reduces the phase-dependent interaction between vortex chains,[8] making them less enduring under thermal fluctuations. In the weak-pinning limit, where a depinned floating state can occur, the corresponding phase diagram becomes rather complicated, due to the possibility of transitions between floating solid and pin solid phases.[22]

In the present paper we study the influence of a periodic pinning substrate on the vortex state in 2D, extreme type-II superconductors, at perpendicular high magnetic fields. Our approach is based on the previously developed theory of vortex lattice melting in pure superconductors,[1,7,8] carried out in the high-magnetic-field limit within the framework of the GL theory in the lowest Landau level (LLL) approximation. Specializing the calculation for a vortex system interacting with a square pinning array under the first matching magnetic

field, we study in detail some key limiting regions of the vortex phase diagram, which enables us to determine its main qualitative features.

II. MODEL

We consider a 2D superconductor at high perpendicular magnetic field, interacting with a periodic substrate of pinning centers, located at (x_i, y_j). A phenomenological Ginzburg-Landau functional, with an order parameter $\psi(x,y)$ in the LLL approximation, is used to describe the SC part of the free energy,

$$H_{sc}=\int dxdy\left[-\alpha|\psi(x,y)|^2+\frac{1}{2}\beta|\psi(x,y)|^4\right], \qquad (1)$$

where α and β are phenomenological parameters.

A local periodic pinning potential[24]

$$V_{pin}=v_0\sum_{i,j}|\psi(x_i,y_j)|^2 \qquad (2)$$

describes the interaction of the vortices with pinning centers. We assume $v_0>0$, so that the pinning energy is minimal if the vortex core positions, determined by $\psi(x_i,y_j)=0$, coincide with pinning centers.

Our main interest here is in the influence of the pinning potential on the vortex lattice melting process, so that the pinning energy V_{pin} is restricted to the range of the vortex lattice melting energy, which is much smaller than the SC condensation energy. Since the latter is of the same magnitude as the cyclotron energy, it is justified to restrict the analysis to the LLL of the corresponding SC order parameter, which can be therefore written as a linear combination of ground Landau orbitals:

$$\psi(x,y)=\sum_n c_n\phi_{q_n}(x,y),$$
$$c_n=|c_n|e^{i\varphi_n},\quad \phi_q(x,y)=e^{2iqx-(y+q)^2}, \qquad (3)$$

where $q_n=qn$, $q=\pi/a_x$, and the amplitudes c_n in the mean-field approximation are related to the (spatial) mean-square SC order parameter Δ_0^2 through $|c_n|^2=c_0^2=\sqrt{(2q^2/\pi)}\Delta_0^2$. In our notation all space variables are measured in units of magnetic length.

In this model, due to the Gaussian attenuation along the y axis over a characteristic distance of the order of the magnetic length, the vortex cores [located at the zeros of $\psi(x,y)$] form a network of linear chains along the x axis, each of which is determined mainly by a superposition of two neighboring Landau orbitals.[8] The parameter a_x is therefore equal to the intervortex distance within a chain, while π/a_x is the interchain spacing in the y direction (see Fig. 1). It should be noted that deviations of Landau orbital (LO) amplitudes from their mean-field value c_0, resulting in strong local distortions of the superfluid density and a large increase of the corresponding free energy density, are neglected in comparison with variations of the phase variables φ_n, provided the orbital direction is selected to be along the principal crystallographic axis.[7,8]

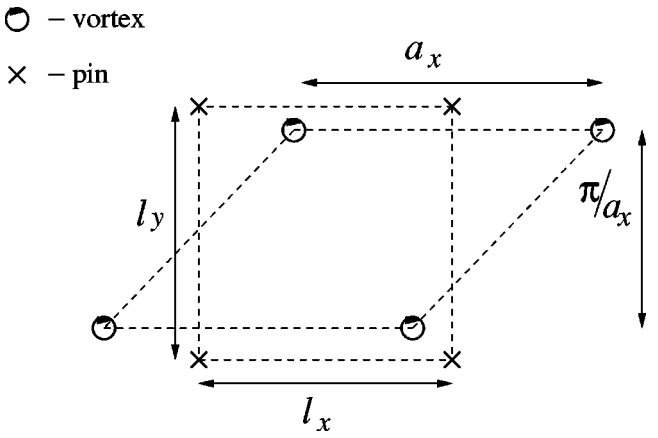

FIG. 1. Schematic arrangement of a vortex lattice (circles) relative to the pin lattice (crosses).

We select the pinning centers to form a rectangular lattice

$$(x_i,y_j)=(l_x i+x_0, l_y j+y_0), \qquad (4)$$

where $i,j=0,\pm1,\ldots$. The parameters x_0 and y_0 determine the relative position of the pin and vortex lattices. The nature of the vortex state in the presence of the pinning potential depends crucially on the ratio of the number of vortices, $N=\sqrt{N}\times\sqrt{N}$, to the number of pinning centers, $N_p=N_{p,x}\times N_{p,y}$. Since the density of vortices depends on the external magnetic field strength H, one can tune this ratio by varying H. Of special interest are the matching fields $H=H_\nu$, $\nu=1,2,\ldots$, when the ratio $n_\phi\equiv N/N_p=\nu$ is an integer.

In matching fields one may distinguish between two different situations, when vortices are bound or unbound to pinning centers. If the pin lattice and vortex lattice unit cells are commensurate along both x and y directions—i.e., $l_x=c_x a_x$, $l_y=c_y\pi/a_x$, with c_x and c_y being integers—the pinning energy is equal to zero, since all the vortices coincide with pinning centers. In all other cases of matching fields, $c_x c_y=\pi\times$integer, none of the numbers $c_x\geqslant1$ and $c_y\geqslant1$ can be integer, and the lattice constants are incommensurate in both directions. It will be shown below that such a vortex configuration is in a floating state with respect to the pin lattice, similar to vortex states in mismatching magnetic fields.

Using the LO representation, Eq. (3), of the SC order parameter in Eq. (2) for the pinning energy, one may take advantage of the localized nature of the LO's and expand V_{pin} in the small parameter $\lambda=e^{-q^2}$, which reflects the small overlap integral between adjacent orbitals contributing to the local superfluid density at the pinning centers. Retaining only dominant terms in λ, Eq. (2) is reduced to the form

$$V_{pin}=V_0\sqrt{\frac{2q^2}{\pi}}\sum_k\left[u_k+2\sum_{m=1}e^{-q^2m^2/2}u_{k+m/2}\Phi_{k,m}\right]$$
$$\simeq V_0\sqrt{\frac{2q^2}{\pi}}\sum_k\left[u_k+2e^{-q^2/2}u_{k+1/2}\Phi_{k,1}\right],$$

$$u_{k+m/2}=\frac{1}{N_{p,y}}\sum_j e^{-2[y_j+q(k+m/2)]^2},$$

$$\Phi_{k,m}=\frac{1}{N_{p,x}}\sum_i \cos(\varphi_{k+m}-\varphi_k+2mqx_i), \tag{5}$$

where $V_0=v_0\Delta_0^2 N_{p,x}N_{p,y}$. It should be stressed that this approximation is valid only for LO's along the principal axes since the minimal distance between them, $q=\pi/a_x$, is sufficiently large to ensure a small and rapidly decreasing value of the overlap integrals between more distant orbitals.

If c_x is not an integer—namely the rectangular pin lattice and vortex lattice are incommensurate in the x direction—then Eq. (5) shows that $\Phi_{k,m}=0$. In this case the pinning energy does not depend on the phases (i.e., the relative horizontal positions) of the Landau orbitals.

Expressing the functions u_k and $u_{k+1/2}$ with the help of a Poisson summation formula as

$$\begin{aligned}u_{k+m/2}&=\frac{1}{N_{p,y}}\sum_j e^{-2[l_y j+y_0+q(k+0.5)]^2}\\&\approx\frac{1}{N_{p,y}}\sqrt{\frac{\pi}{2l_y^2}}\Bigg[1+2\sum_j e^{-\pi^2 j^2/2l_y^2}\\&\quad\times\cos\left(\frac{2\pi j[q(k+m/2)+y_0]}{l_y}\right)+\cdots\Bigg],\end{aligned} \tag{6}$$

we note that when the lattices are incommensurate also along the y axis (i.e., when both c_x and c_y are not integer) the oscillating terms in u_k are averaged to zero after summation over k. Thus, the pinning energy for incommensurate lattices is a constant:

$$V_{pin}=V_0\frac{q\sqrt{N}}{l_y N_{p,y}}=V_0, \tag{7}$$

which does not depend on the mutual orientation of the vortex and pin lattices. Note that the system size in the y direction is $L_y=q\sqrt{N}=l_y N_{p,y}$, a relation connecting $\sqrt{N}$ to $N_{p,y}$. The obtained result is valid only for a large system, $N\to\infty$, where the boundary effect can be neglected.

For the sake of simplicity, we will consider in what follows a square pin lattice with $n_\phi=1$. In the commensurate situation the pinning energy is minimal (i.e., equal to zero) when all vortices coincide with pinning centers. Deviations of vortices from this configuration in the form of shear distortions along the principal crystallographic axes are of special interest due to the relatively low SC energy involved. For the principal axis parallel to a side of the square unit cell, $c_x=c_y=1$ and $q^2=\pi$, and so, according to Eq. (5), the pinning energy per single vortex is, up to small terms of the order $\sim e^{-2\pi}$, given by

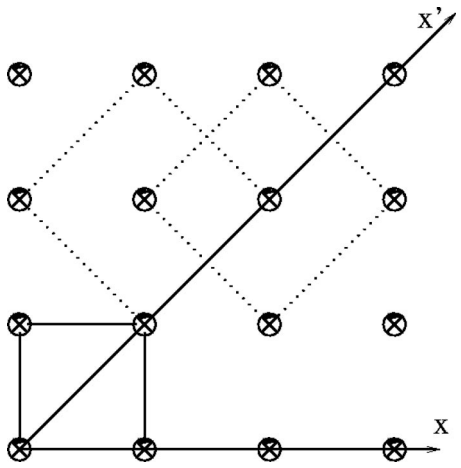

FIG. 2. Primitive and nonprimitive unit cell representations (solid and dotted lines, respectively) of the square pin lattice used for a description of the shear distortion along the principal axes of the vortex lattice. Similar to Fig. 1, ○ and × denote vortex and pinning center positions, respectively. Vectors x and x' show the directions of the principal axes.

$$\begin{aligned}\frac{V_{pin}}{N}&=v\frac{1}{\sqrt{N}}\sum_k\left[a_1-a_2\cos(\varphi_k-\varphi_{k-1})\right]\\&\simeq\kappa_x v\frac{1}{\sqrt{N}}\sum_k\left[1-\cos(\xi_k)\right],\end{aligned} \tag{8}$$

where $v=V_0/N$, $a_1=1-2e^{-\pi/2}\simeq 0.584$, and $a_2=2e^{-\pi/2}(1+2e^{-\pi/2})\simeq 0.589$. Note that in the above expressions we set $x_0=y_0=q/2$ so that the minimal pinning energy is obtained for $\xi_k=0$. Note also that for the undistorted square lattice in which $\varphi_k=\varphi_{k-1}$, the expression in the first line of Eq. (8) is not strictly zero since $a_1\neq a_2$. The error, which is of order higher than the second in $e^{-\pi}$, can be neglected in the approximation leading to Eq. (8). The numbers a_1, a_2 can be thus considered equal within this approximation, allowing us to introduce a single coefficient $\kappa_x\equiv a_1\simeq a_2\simeq 0.59$. The expression in the second line of Eq. (8) yields the correct (i.e., zero) value for the undistorted lattice. It is written in terms of the variables $\xi_k\equiv\varphi_k-\varphi_{k-1}$ describing the lateral positions of the vortex chains, which are generated mainly by interference between two neighboring LO's. This is consistent with the well-known definition $u_x=\partial\varphi/\partial y$ of vortex displacement along the x axis in the long-wavelength limit.[25]

To evaluate the excess pinning energy associated with shear distortion along the diagonal of the square unit cell the pin lattice may be conveniently described by two interpenetrating simple square sublattices with $c_x=1$, $c_y=2$, and $q^2=2\pi$ (see Fig. 2). The corresponding interchain pinning energy for each of the sublattices can again be obtained from Eq. (8), with $\kappa_{x'}\simeq 0.84$ and a phase shift of $\pi/2$, which arises due to different shape of the unit cell.

The SC part of the free energy functional, for the commensurate lattices described above, is then calculated by substituting the order parameter, Eq. (3), in Eq. (1), with the inter-Landau-orbital distance set equal to the lattice constant

of the square pin lattice ($a_x=\sqrt{\pi}$) and with the orbital amplitudes $|c_n|$ assuming the value given by the mean-field approximation. Expanding the resulting expression in the small parameter $\lambda_{sq}=\exp(-\pi)$, which characterizes interorbital coupling,[7] and truncating the resulting expansion at the leading phase-dependent term ($\sim\lambda_{sq}^2$) yields the following (ξ_k-dependent) expression:

$$\frac{H_{sc}}{N}=-h_{\square}-T_{\square}\frac{1}{\sqrt{N}}\sum_k\ [1-\cos(\xi_{k+1}-\xi_k)], \qquad (9)$$

where $h_{\square}$ is the SC condensation energy (per unit flux) of the square vortex lattice and $T_{\square}=[4\lambda_{sq}^2/(1+4\lambda_{sq})]h_{\square}$ is the shear distortion energy parameter. Here $h_{\square}=\varepsilon_0\beta_A/\beta_{sq}$, where $\beta_A\simeq 1.159$ and $\beta_{sq}\simeq 1.18$, are the values of the Abrikosov structure parameter for regular hexagonal and square lattices, respectively, and $\varepsilon_0\equiv\pi\alpha^2/2\beta_A\beta$ is the SC condensation energy of the former.

For the specific choice $\xi_k=\gamma k$, where γ is a constant, the Bragg family of vortex chains along the principal axis, denoted *x*, is characterized by a lateral displacement $\xi_{k+1}-\xi_k=\gamma$ between neighboring chains. Evidently, the SC energy H_{sc} for the undistorted square vortex lattice $\xi_k=0$ ($\gamma=0$) [see Eq. (9)] is equal to $Nh_{\square}$. However, the minimum of the SC energy with respect to the collective tilt angle parameter γ is reached for a triangular vortex lattice, determined by $\xi_k=\pi k$ ($\gamma=\pi$), whose unit cell is an isosceles triangle with a base (along the *x* axis) and a height equal to $\sqrt{\pi}$ (see Fig. 3). The corresponding SC energy is equal to $H_{sc}/N=-h_{\square}-2T_{\square}$. This value is lower than the SC energy of the square vortex lattice and only slightly higher (i.e., by $\sim 0.45\%$) than the SC energy of the equilateral triangular (Abrikosov) lattice, $H_{\triangle}/N=-\varepsilon_0$.

III. VORTEX STATES FOR THE LOWEST MATCHING FIELD

A. Commensurate and incommensurate ground states

The competition between the pinning energy, Eq. (8), which favors vortices approaching the pinning points on a square lattice, and the SC energy, Eq. (9), preferring triangular lattice configuration, leads to ''frustrated'' vortex structures, which depend on the relative pinning strength.

At zero temperature they can be obtained by minimizing the total energy, consisting of the SC and pinning parts. Since in the LO representation each orbital is $\sqrt{N}$-fold degenerate, the effective Hamiltonian is written as

$$f_{\square}=\frac{H_{sc}+V_{pin}}{N}=\frac{T_{\square}}{\sqrt{N}}\sum_k\ \{-h_{\square}/T_{\square}+4p[1-\cos(\xi_k)]$$
$$-[1-\cos(\xi_{k+1}-\xi_k)]\}, \qquad (10)$$

where the parameter $p\equiv\kappa_x v/4T_{\square}$ determines the strength of the pinning potential relative to the inter-vortex-chain coupling. Under the constraints imposed by the requirement of commensurability between the vortex configuration and pin lattice, the vortex chains are restricted to move laterally along the common *x* axis of the underlying lattices (see Fig. 1). The corresponding displacements ξ_k may be separated into two groups, corresponding to even and odd vortex chains, as follows:

$$\xi_k=\begin{cases}\theta_l & \text{for} \quad k=2l,\\ \zeta_l & \text{for} \quad k=2l-1,\end{cases} \qquad (11)$$

so that

$$f_{\square}=\frac{T_{\square}}{\sqrt{N}}\sum_l\ \{-2h_{\square}/T_{\square}+4p[2-\cos(\theta_l)-\cos(\zeta_l)]$$
$$-[2-\cos(\theta_l-\zeta_l)-\cos(\theta_{l-1}-\zeta_l)]\}. \qquad (12)$$

The calculation may be greatly simplified if we assume that the stationary point values within each group are all equal: that is, $\theta_l=\theta_c$ and $\zeta_l=\zeta_c$. This restriction may be justified in the weak-pinning regime $0<p<1$, where the dominant SC energy part favors periodic triangular vortex structures, as shown in Fig. 3(a).

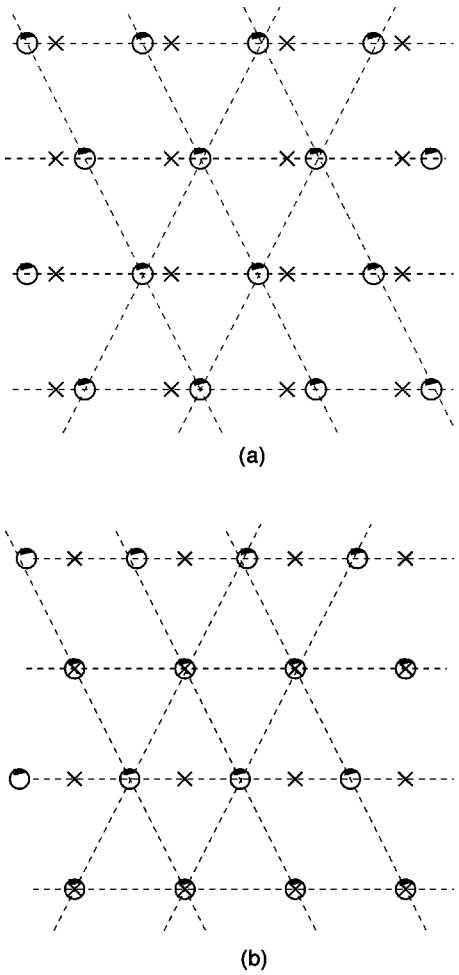

FIG. 3. (a) The vortex lattice state with the lowest energy, which is commensurate with a square pinning lattice in the limit of zero pinning strength. (b) An alternative vortex lattice state, which may be favorable under square framework boundary conditions (see text). In the figure ○ and × are vortices and pins, respectively.

Substituting these values into Eq. (12) and minimizing the resulting functional one finds that the total energy has a minimum

$$\min(f_{\square}) = -\frac{1}{\sqrt{N}} \sum_{k} [2T_{\square}(1-p)^2 + h_{\square}] \qquad (13)$$

at $\theta_c = -\zeta_c = \theta_0$ where

$$\cos(\theta_0) = p. \qquad (14)$$

Thus, at zero pinning strength $p=0$, the ground-state energy per unit flux, $f_{\square} = -2T_{\square} - h_{\square}$, corresponds to a triangular vortex lattice configuration $\theta_c = -\zeta_c = \pi/2$, whereas in the opposite extreme, when $p=1$, the ground-state energy $f_{\square} = h_{\square}$ corresponds to a square vortex lattice $\theta_c = -\zeta_c = 0$, which coincides with the underlying pin lattice. It should be stressed, however, that due to the constraints imposed by the requirement of commensurability with the pin square lattice, the triangular vortex structure obtained in the zero-pinning-strength limit is not the equilateral (Abrikosov) lattice [see Fig.3(a)]. This discontinuity indicates that the transition to the depinned (floating) vortex lattice should be of the first order (see below).

An illustration of the weak-pinning ground-state configuration is shown in Fig. 3(a). It is seen that odd and even vortex chains are shifted in opposite directions symmetrically with respect to the underlying substrate. The relative positions of the two lattices are determined by the strength of the pinning potential, V_0. In the zero-pinning limit $V_0 \to 0$, the vortices in odd (even) chains approach lattice points which are shifted laterally by a quarter of a lattice constant, $\frac{1}{4} l_x$ ($l_x = \sqrt{\pi}$), in the positive (negative) sense with respect to the square pin lattice, forming isosceles triangular lattice. Note that the asymmetric configuration, shown in Fig. 3(b), in which half of the vortex chains remain pinned to the underlying substrate, has energy $-2T_{\square}(1-2p) - h_{\square}$, which is only slightly (i.e., by a small, second-order correction in p) higher than the energy given by Eq. (13). Such an asymmetric configuration may become energetically favorable (see Refs. 22 and 23) due to, e.g., boundary conditions which are incompatible with the even-odd chain symmetry described above.

At sufficiently weak pinning, when the pinning energy becomes comparable to the difference between the SC energies of the commensurate isosceles triangular vortex lattice with $a_x^2 = \pi$ and the incommensurate equilateral triangular lattice with $a_x^2 = \sqrt{3}\pi/2$ (Abrikosov lattice), the latter is preferable. To show this note that the energy $-h_{\triangle}$ of the equilateral triangular vortex lattice in the presence of incommensurate pin lattice is influenced only by the average pinning potential v, so that

$$-h_{\triangle} = -\varepsilon_0 + v = -\varepsilon_0 + \frac{4}{\kappa_x} p T_{\square}. \qquad (15)$$

Comparing this value with that obtained in Eq. (13) for the commensurate, isosceles triangular lattice, $-2T_{\square}(1-p)^2 - h_{\square}$, we find that for $p \leqslant p_c \simeq 0.25$ the floating equilateral triangular lattice is the lowest-energy state. This critical point can be thus identified as a transition point from a pinned (commensurate) solid to a floating (incommensurate) solid state.

A second critical point exists in the strong-pinning regime—i.e., at $p=1$—as indicated by Eq. (14), which has no real solution at any $p>1$. At this critical point the vortex lattice coincides with the square pin lattice [i.e., $\theta_0 = 0$ in Eq. (14)] and the pinning energy reaches its absolute minimum value (i.e., zero). Since any further increase of the pinning strength above the critical value, $p=1$, cannot be compensated by the SC energy terms in Eq. (12), the vortex configuration remains fixed at the square lattice structure for any $p \geqslant 1$. Thus, with increasing values of the parameter p, the ground-state vortex configuration changes continuously from a triangular lattice at $p = p_c$ to a square lattice at $p=1$, which does not changes with further increase of the pinning strength. This continuous transformation from a triangular lattice to a square lattice can be classified as a second-order phase transition at $p=1$.

B. Commensurate equilibrium states at finite temperature

In the ideal vortex state at finite temperature thermal fluctuations associated with the low-lying shear excitations along the principal crystallographic axis destroy the long-range phase coherence of the vortex state and lead to melting of the ideal vortex lattice at a temperature T_m well below the mean field T_c. This feature indicates an intrinsic anisotropy of the ideal vortex crystal[8]: The characteristic excitation energy for sliding vortex chains along the principal axis (denoted by x) parallel to a side of the unit cell (see Fig. 2) is two orders of magnitude smaller than the SC condensation energy and one order of magnitude smaller for fluctuations along the diagonal axis (denoted by x'). For all other crystallographic orientations the shear energy is of the order of the SC condensation energy.

The nucleation of a SC crystallite can be established in such an ideal model by selecting boundary conditions which fix the position of a single-vortex chain with respect to the laboratory frame. As shear fluctuations of parallel vortex chains diverge with the distance from the fixed chain,[7] a SC domain is restricted to nucleate only around a pinned chain, its transverse size shrinking to that of a single magnetic length as the temperature rises toward T_m. For the sake of simplicity, we avoid here the complication associated with the discontinuous nature of the vortex lattice melting process, which involves two principal families of easily sliding Bragg chains,[1] and restrict the analysis to a single family of vortex chains: i.e., that with the lowest crossover temperature T_{cm} (Ref. 8). A meaningful definition of $T_{cm}(a_x)$ may invoke the phase correlation function

$$C_{n',n} \equiv \langle e^{i(\varphi_{n'} - \varphi_n)} \rangle \qquad (16)$$

between Landau orbitals n' and n located near the fixed chain $n=0$. Thus, melting of the entire vortex lattice occurs essentially when phase correlation between the nearest-neighboring chains (i.e., $n=1$, $n'=2$) closest to the fixed

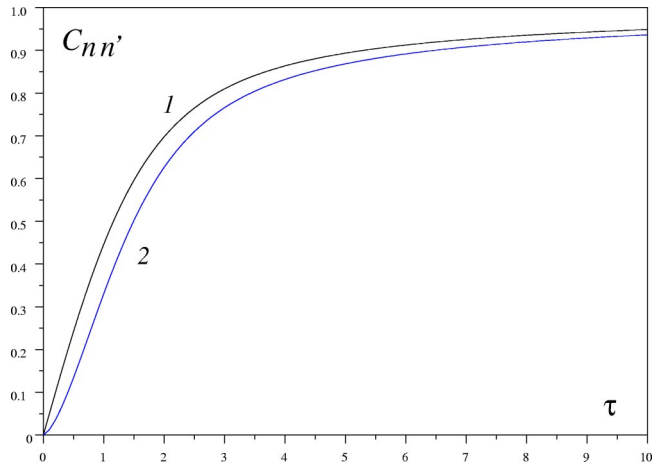

FIG. 4. Pair correlation function between nearest Landau orbitals: (1) at strong pinning, as a function of the dimensionless inverse temperature $\tau=4pT_{\square}/T$, and (2) in the triangular Abrikosov vortex lattice with a single pinned chain, $n=0$, as a function of $\tilde{\tau}\equiv T_{\triangle}/T$.

chain is significantly suppressed (e.g., by a factor of 1/2). In the $p\to 0$ limit we use the expression derived in Ref. 7 to find

$$C_{n'=2,n=1}(\tilde{\tau})\simeq\left(\frac{I_1(\tilde{\tau})}{I_0(\tilde{\tau})}\right)\left(\frac{I_{1/2}(\tilde{\tau})}{I_0(\tilde{\tau})}\right),$$

with $\tilde{\tau}\equiv T_{\triangle}/T$. Here the characteristic temperature $T_{\triangle}\simeq[4\lambda^2/(1+4\lambda)]\varepsilon_0$ with $\lambda=\exp(-\sqrt{3}\pi/2)$, corresponds to an interaction between the principal LO's in the equilateral triangular lattice state. Note that the crossover between the vortex solid state at zero temperature, where $\tilde{\tau}\to\infty$ and $C_{n'=2,n=1}(\tilde{\tau})\to 1$, and the vortex liquid state at high temperature, where $\tilde{\tau}\to 0$ and $C_{n'=2,n=1}(\tilde{\tau})\to 0$, occurs at about $\tilde{\tau}\simeq 1.5$, so that $T_{cm}(a_x)\approx 0.67T_{\triangle}$ (see Fig. 4). This crossover temperature is close to, though somewhat lower than, the melting temperature $T_m\simeq 1.2T_{\triangle}\simeq 2.8T_{\square}$ predicted in Ref. 7.

The presence of the periodic pinning potential stabilizes the vortex lattice against the violent phase fluctuations discussed above. This effect is nicely demonstrated by the phase correlation function $C_{n',n}$ [Eq. (16)], which controls the mean superfluid density [see Eq. (3)] near the melting point. Assuming strong pinning $p\gg 1$ and neglecting the small GL inter-vortex-chain coupling, the correlation function can be determined from the expression

$$C_{n',n}\simeq\frac{\prod_k\int_0^{\pi}d\xi_k e^{i(\varphi_{n'}-\varphi_n)}e^{-4p\tau\cos(\xi_k)}}{\prod_k\int_0^{\pi}d\xi_k e^{-4p\tau\cos(\xi_k)}}. \qquad (17)$$

Using the identity $\varphi_n=\Sigma_{k=n_0}^{n}\xi_k$, where the value of n_0 can be found from boundary conditions which influence only the global phase of the SC order parameter, we find that

$$C_{n',n}\simeq\left(\frac{I_1(4p\tau)}{I_0(4p\tau)}\right)^{|\Delta n|}\simeq\exp(-|\Delta n|/8p\tau)\quad\text{for}\quad 4p\tau\gg 1, \qquad (18)$$

where $\Delta n\equiv n'-n$. This result contrasts with the correlation function obtained in the pure state,[7] which has the asymptotic form

$$C_{n',n}\propto\exp\left(-\frac{\overline{n}}{2\tau}|\Delta n|^2\right)\quad\text{for}\quad\tau\gg 1, \qquad (19)$$

where $\overline{n}=n'/3+2n/3-1/2$, with the $n=0$ chain being fixed. As discussed above (see also Refs. 1, 7 and 8), fixing chain positions through boundary conditions is physically equivalent to introducing a pinning potential into the GL functional, which is a crucial step for stabilizing the vortex lattice. The global stability of the vortex lattice in the presence of the periodic pinning potential is reflected in Eq. (18), as compared with Eq. (19), by the translational invariance of the former correlation function, as well as by its relatively weak (simple exponential) decay.

To determine the crossover temperature from the square pin solid (SPS) to the vortex liquid we may follow the procedure described above and find the temperature $T_{cm}(a_x,p)$ at which $C_{n',n}$ in Eq. (17) for $|\Delta n|=1$ is reduced by a factor of 1/2 with respect to its zero-temperature ($\tau\to\infty$) limit. This yields in the strong-pinning limit $p\gg 1$ (see Fig. 4) the linear dependence

$$T_{cm}(a_x,p)\approx 0.86\times 4pT_{\square}. \qquad (20)$$

Beside its influence on the vortex lattice melting transition, the pinning potential can change the vortex lattice structure, both continuously and discontinuously. The zero-temperature limit was discussed in Sec. III A. Above the critical value $p=1$ the lateral vortex positions coincide with the pin square lattice positions, $\xi_l=0$. For decreasing pinning strength below $p=1$, the configuration of the vortex lattice deviates continuously from the square structure to a lattice with vortices shifted along chains away from the pinning centers.

A similar second-order SPS to triangular pin solid (TPS) phase transition (as a function of p) is expected at finite temperatures. Indeed, as shown in Sec. III A, the free energy functional $f_{\square}$ in Eq. (10) is minimized at the stationary points $\xi_k=\xi_{ck}\equiv(-1)^k\theta_0$, with $\cos\theta_0=p$ for $p\leqslant 1$, and at $\xi_{ck}=0$ for $p\geqslant 1$. Thus, expanding $f_{\square}$ as a Taylor series in $(\xi_k-\xi_{ck})$ about its stationary points it is clear that for $p\geqslant 1$ (when $\xi_{ck}=0$) the expansion includes only *even* powers ξ_k (due to the symmetry of $f_{\square}$ with respect to $\xi_k\to-\xi_k$). Thus, at any finite temperature T, the thermal mean values $\langle\xi_k\rangle$ are equal to zero for $p\geqslant 1$, implying that for pinning strengths above the critical value $p=1$ the mean vortex positions coincide with the square pin lattice.

IV. PHASE DIAGRAM FOR THE LOWEST MATCHING FIELD

The results of the previous sections enable us to draw a rather clear picture of the p-T phase diagram, as shown in

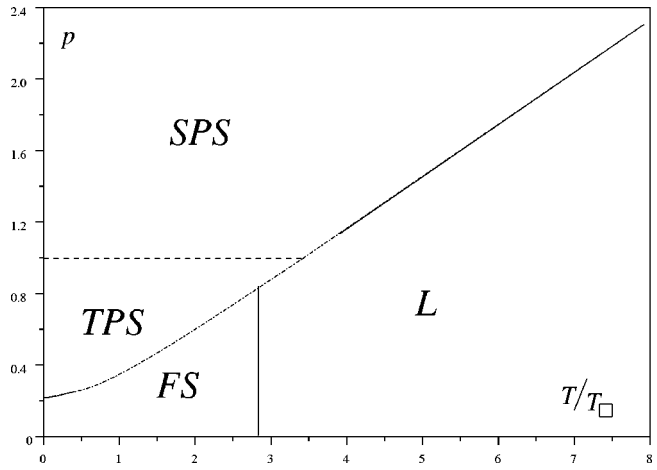

FIG. 5. p-T phase diagram. Solid lines: first-order phase transitions from SPS to L phase (at large pinning strength), from TPS to FS (near zero temperature), and between FS and L phases. Dashed line: second-order phase transition between partially pinned (TPS) and fully pinned (SPS) vortex crystals. The dash-dotted line connects smoothly between the asymptotic SPS-L line and the low-temperature TPS-FS line (see text for explanation).

Fig. 5. In the strong-pinning regime, $p \gg 1$, the pinning strength is so large that the gain in commensurate energy is larger than the vortex-vortex energy gain at any temperature, and so the floating solid (FS) phase is not favorable. Thus, the vortex lattice melting in this region should take place directly from the SPS to the liquid (L) phase, as described by the asymptotic expression, Eq. (20), which is equivalent to the straight line $p \approx 0.29 T/T_{\square}$ in the large-p regime of the phase diagram.

In the small-p regime the stable phase at low temperatures is the FS. Here the energy gain associated with creation of the close-packed equilateral triangular vortex lattice exceeds the energy cost of the incommensurate state. This state remains stable up to a relatively high temperature $T \simeq 2.8 T_{\square}$, above which it melts into a vortex liquid state. The phase boundary in this region is vertical (i.e., independent of p) since it is determined by the vortex-vortex coupling and not by the pinning energy (which is a constant in the floating state).

In the low-temperature region of the phase diagram our analysis shows the existence of two phase transitions: At small pinning, increasing p above $p_c \approx 0.25$ transforms the FS discontinuously to a pin solid since the energy gain associated with the commensurate pin vortex solid exceeds the energy cost of distorting the close-packed equilateral triangular vortex lattice. The discontinuous nature of this transition is due to the fact that even an infinitesimal deviation from a commensurate configuration raises the pinning energy by a finite amount (i.e., at least from $0.6v$ to v).

It turns out that the pin vortex crystal just above the commensurate-incommensurate transition is not a square lattice, as found by Reichhardt *et al.*,[22] but a triangular one, with a unit cell which depends on the pinning strength. At $T=0$ it is a parallelogram with equal base and height, which transforms continuously to a square at $p=1$. A similar continuous transition from a frustrated triangular pin lattice to the SPS takes place at the critical pinning strength $p=1$ at any temperature T. Interestingly, the corresponding horizontal transition line intersects the extrapolated SPS-L boundary line at $T \approx 3.44 T_{\square}$, $p=1$, that is in the close vicinity of the intersection between the vertical FS melting line, $T \simeq 2.8 T_{\square}$, and the SPS-TPS line.

It is not exactly known, however, how the FS-TPS boundary is extended beyond the zero-temperature region. It is conceivable that its high-temperature sector coincides with the low-temperature sector of the SPS melting line. This is due to the fact that, at a fixed value of p, the driving force for both transitions is thermal fluctuations involving sliding vortex chains, which suppress the pinning energy gained in the commensurate phase [i.e., the term $-4p\cos(\xi_k)$ in Eq. (10)]. In the SPS-L transitions, where the vortex-vortex interaction is relatively small, this suppression leads to uncorrelated vortex chains, resulting in melting. In the TPS-FS transitions, where the vortex-vortex coupling is relatively large, the suppression of the pinning energy results in mutually correlated vortex chains, which lose correlation with the underlying pinning lattice.

An intermediate pin solid phase of a triangular form has been also found in the London model calculation reported by Pogosov *et al.*[23] However, in contrast to the Ginzburg-Landau model, discussed here, they predicted the vortex configurations shown in Fig. 3(b) as preferable below some critical value of the pinning potential strength. Above this value the symmetry of vortex lattice is changed discontinuously to the square symmetry of the pin lattice.

Our proposed phase diagram, shown in Fig. 5, thus consists of two pin solid phases, a floating solid and a liquid phase, delimited by four interphase boundary lines, which intersect at two nearby triple points. This result is similar to the phase diagram found by Reichhardt *et al.*[22] using molecular dynamics simulations. However, the intermediate TPS phase obtained in our calculation is missing in Reichhardt *et al.* This seems to be due to the different limiting situations studied in the two works. The present approach is valid for high magnetic fields (i.e., when the intervortex distance is much smaller than the London penetration depth) while the approach of while Reichhardt *et al.* was applied for low and moderate magnetic fields (when the intervortex distance is of the order of the penetration depth). Consequently in the latter model the effective vortex-vortex interaction strength is much weaker than in the former and so could influence the PS-FS phase boundary only at extremely low pinning strengths, which were not studied in the numerical calculation of Ref. 22. This accounts also for the different zero-temperature limits of the PS-FS line in the two works, which is seen to approach $p=0$ in Reichhardt *et al.*

V. CONCLUSIONS

The influence of a periodic pinning potential on the vortex state of a 2D superconductor at temperatures well below the mean field T_c has been studied within the framework of the GL functional integral approach. It is shown that an attractive interaction of vortex cores to a commensurate pin lattice stabilizes vortex solid phases with long-range positional or-

der against violent shear fluctuations along the principal crystallographic axis. Exploiting a simple analytical approach we draw a rather detailed picture of the relevant vortex-state p-T (pinning strength and temperature) phase diagram. In agreement with previous numerical simulations,[22] we have found a pinned, commensurate solid phase in the strong-pinning and low-temperature part of the phase diagram, which melts into a vortex liquid at high temperatures and transforms into a floating (incommensurate) solid at low temperatures. We have shown that at low temperature, similar to Ref. 23, there is an intermediate triangular phase, where vortices detaching from pinning centers remain strongly correlated with them. This pinned (frustrated) triangular solid transforms continuously into the fully pinned (square) solid phase at $p=1$ and discontinuously to a floating solid at small pinning strengths. The zero-temperature limit of this commensurate-incommensurate transition line occurs at a finite pinning strength ($p=p_c\approx 0.25$).

It is predicted that for sufficiently clean samples, where random pinning is weak enough, application of an artificial periodic pinning array with an appropriate strength would stabilize a weakly pinned vortex solid phase with long-range positional order. Exploiting the SANS method to the sample under these conditions one could therefore directly detect the shear stiffness anisotropy characterizing the ideal vortex lattice.

ACKNOWLEDGMENT

This research was supported in part by a grant from the Israel Science Foundation founded by the Academy of Sciences and Humanities and by the fund from the promotion of research at the Technion.

*Electronic address: maniv@tx.technion.ac.il

[1] T. Maniv, V. Zhuravlev, I.D. Vagner, and P. Wyder, Rev. Mod. Phys. **73**, 867 (2001).
[2] S. Doniach and B.A. Huberman, Phys. Rev. Lett. **42**, 1169 (1979).
[3] Daniel S. Fisher, Phys. Rev. B **22**, 1190 (1980).
[4] J.M. Kosterlitz and D.J. Thouless, J. Phys. C **6**, 1181 (1973); B.I. Halperin and D. Nelson, Phys. Rev. Lett. **41**, 121 (1978); A.P. Young, Phys. Rev. B **19**, 1855 (1979).
[5] Z. Tesanovic and A.V. Andreev, Phys. Rev. B **49**, 4064 (1994).
[6] J. Hu and A.H. MacDonald, Phys. Rev. B **56**, 2788 (1997).
[7] V. Zhuravlev and T. Maniv, Phys. Rev. B **60**, 4277 (1999).
[8] V. Zhuravlev and T. Maniv, Phys. Rev. B **66**, 014529 (2002).
[9] A.T. Fiory, A.F. Hebard, and S. Somekh, Appl. Phys. Lett. **32**, 73 (1978).
[10] M. Baert, V.V. Metlushko, R. Jonckheere, V.V. Moshchalkov, and Y. Bruynseraede, Phys. Rev. Lett. **74**, 3269 (1995).
[11] A. Castellanos, R. Wordenweber, G. Ockenfuss, A.v.d. Hart, and K. Keck, Appl. Phys. Lett. **71**, 962 (1997).
[12] V.V. Moshchalkov, M. Baert, V.V. Metlushko, E. Rossel, M.J. Van Bael, K. Temst, Y. Bruynseraede, and R. Jonckheere, Physica C **332**, 12 (2000).
[13] J.I. Martin, M. Velez, J. Nogues, and I.K. Schuller, Phys. Rev. Lett. **79**, 1929 (1997).
[14] D.J. Morgan and J.B. Ketterson, Phys. Rev. Lett. **80**, 3614 (1998).
[15] M.J. Van Bael, K. Temst, V.V. Moshchalkov, and Y. Bruynseraede, Phys. Rev. B **59**, 14 674 (1999).
[16] A. Terentiev, D.B. Watkins, L.E. De Long, L.D. Cooley, D.J. Morgan, and J.B. Ketterson, Phys. Rev. B **61**, R9249 (2000).
[17] D.R. Nelson and B.I. Halperin, Phys. Rev. B **19**, 2457 (1979).
[18] L. Radzihovsky, Phys. Rev. Lett. **74**, 4923 (1995).
[19] C. Reichhardt, C.J. Olson, and F. Nori, Phys. Rev. Lett. **78**, 2648 (1997); Phys. Rev. B **58**, 6534 (1998).
[20] V. Marconi and D. Dominguez, Phys. Rev. Lett. **82**, 4922 (1999); C. Reichhardt and G.T. Zimanyi, Phys. Rev. B **61**, 14 354 (2000); G. Carneiro, *ibid.* **62**, R14 661 (2000).
[21] C. Dasgupta and O.T. Valls, Phys. Rev. B **66**, 064518 (2002).
[22] C. Reichhardt, C.J. Olson, R.T. Scalettar, and G.T. Zimanyi, Phys. Rev. B **64**, 144509 (2001).
[23] W.V. Pogosov, A.L. Rakhmanov, and V.V. Moshchalkov, Phys. Rev. B **67**, 014532 (2003); V.N. Rud'ko, O.N. Shevtsova, and S.V. Shiyanovsky, Low Temp. Phys. **22**, 999 (1996).
[24] Z. Tesanovic and I.F. Herbut, Phys. Rev. B **50**, 10 389 (1994).
[25] M.A. Moore, Phys. Rev. B **39**, 136 (1989).